The Effects of the Sol-Gel Transition of Alginates on Effective Charge Densities

Masakatsu YONESE,* Kazuhiko BABA, and Hiroshi KISHIMOTO
Faculty of Pharmaceutical Sciences, Nagoya City University, Tanabe-dori, Mizuho-ku, Nagoya 467
(Received September 28, 1987)

The counterion binding properties of alginate (Alg) sol and gel were studied by using the membrane potential method, in which membranes were constructed of an Alg layer sandwiched between supporting films. The concentrations of Alg W_{Alg} ranged from 0.0025 to 0.0063 g cm^{-3}, and the membrane potentials were measured in NaCl, $MgCl_2$, and $CaCl_2$ solutions. The effective charge densities of Alg (θ^{*2}) were obtained by curve fittings with the theoretical values of the multimembrane potentials. The ratios of θ^{*2} to the concentration of uronate units θ_0 were found not to depend on W_{Alg}; their mean values were 0.45, 0.28, and 0.12 for Na-, Mg-, and CaAlg. The results of Na- and MgAlg in the sol state were bigger than Manning's theoretical values. The much smaller values of CaAlg in the gel state than MgAlg in the sol state showed that the Ca ion binding was enhanced by the gellation not only in the junction, but also in the networks.

Alginate (Alg) is a major structural polysaccharide found in intercelluar substances of brown algae, such as Laminaria hyperbória and Laminaria digitata, and is a linear block copolymer of β-D-mannuronate (M) and its C-5 epimer, α-L-guluronate (G). They link together in an alternative way (MG block) or in consecutive homopolymeric ways (G and M block). The ratio of M and G and the block compositions vary with the sources of brown algaes, and even with the same source, they vary by part and by age.[1] Alginates are gelled by the addition of divalent metal ions M^{++}, except for Mg^{++} ions. The crosslinks are formed by the stackings of the G blocks of alginate chains mediated by M^{++}.[2-4] Differing from thermotropic gels, such as carrageenan, Alg shows a sol-gel transition without any alteration in the temperature.[5] Therefore, it is a very valuable polysaccharide for basic studies of gel and for applications in the pharmaceutical field.[6,7]

The counterion-binding properties of Alg have been studied primarily by means of a dialysis-equilibrium method, and the divalent metal ions inducing its gellation have been reported to bind spcifically.[8-10] To elucidate the counterion-binding properties of Alg in sol and gel states, the membrane potential method[11] was used; in the method, membranes are constructed of an Alg sol and gel layer sandwiched between supporting films. The effective charge densities of Alg are studied. This method makes it possible to study the charge densities of both the sol and the gel, i.e., the effects of the sol-gel transition of Alg on counterion-bindings.

Experimental

Materials. Purified sodium alginate (NaAlg) was prepared from commercial NaAlg (Tokyo Kasei Kogyo Co., Ltd.) by dialyzing it against distilled water for 3 days, followed by filtration to remove any insoluble substances. The NaAlg thus purifed was stored under refrigeration after freeze-drying. The weight average molar mass of NaAlg was determined to be $M_w=1.32\cdot10^5$ g mol^{-1} by using a light scattering photometer LS-8 (Toyo Soda Manufacturing Co., Ltd., Japan). The compositions of NaAlg were analyzed by means of circular dichroism, CD,[12] and ^{1}H NMR.[13] The guluronate fraction F_G was found to be 0.33 or 0.37 by the two methods, while the fraction of the consecutive guluronate block F_{GG} and that of the alternative block composed of guluronate and mannuronate F_{MG} were determined to be 0.28 and 0.18 by ^{1}H NMR. All the other reagents were special grade. Distilled and deionized water was used for the preparation of aqueous solutions.

Measurement of Membrane Potential. In order to estimate the effective charge densities of polyelectrolyte solutions, the membrane potentials were studied by using the multimembrane, shown in Fig. 1 (a), constructed of a poly-

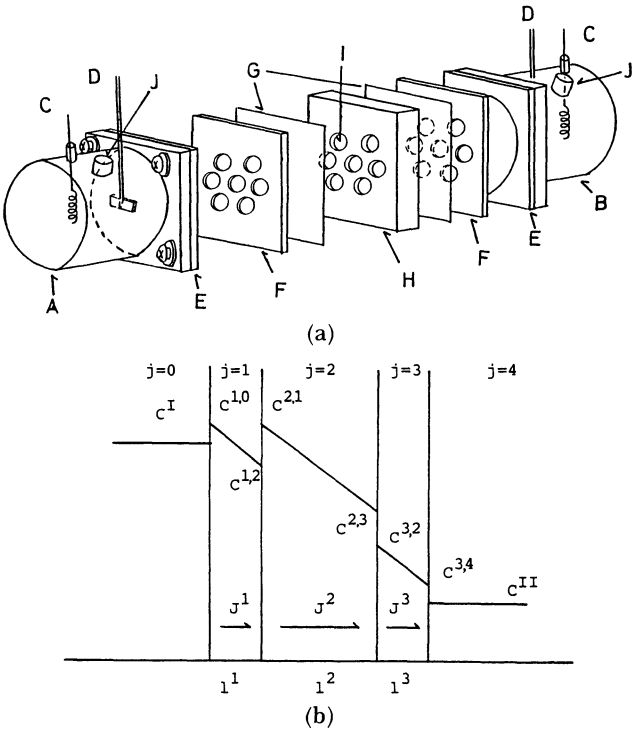

Fig. 1. Schemes of multimembrane. (a) Membrane potential measurement cell. A; compartment I, B; compartment II, C; Ag/AgCl electrode, D; stirring bar, E; silicone rubber, F; perforated stainless steel plate, G; support film (first and third layer), H; perforated polyacrylic resin plate, I; sample injection hole (second layer), J; inlet for solution injection. (b) Notations of concentrations for multimembrane system. $C^{0,1}$ and $C^{4,3}$ denote C^I and C^{II}.

electrolyte solution layer (I) sandwiched between supporting films (G): Solution I |Film| Polyelectrolyte solution layer |Film| Solution II. Dialysis membranes, C.M., (0.0033 cm in thickness, Seamless Cellulose Tubing, Union Carbide Corp.) was used as supporting films. NaAlg solutions were put into holes (I) (0.25 cm in radius) in a perforated polyacrylic resin plate (H) (0.3 cm thick, with 7 holes in it), and the supporting films on both sides were fixed by means of perforated stainless steel plates (F). The concentrations of Alg W_{Alg} were in the range from 0.0025 to 0.00626 g cm^{-3}. The concentration ratios of electrolyte solutions in the Compartments I (A) and II (B), R ($=C^{I}/C^{II}$) were 10 and 2. Both solutions were stirred at 500 rpm by means of stirring bars (D) so as to attain a constant thickness of the stagnant layer (=40 μm), a value which was obtained by measuring the permeability coefficients of NaCl through the single and double dialysis membranes.[14] The membrane potentials E between Solution I and Solution II were measured by means of Ag/AgCl electrodes (C), whose electrode potentials had been obtained by using Kieland's individual activil coefficients.[15] To obtain the effective charge density of the supporting films, C.M., the membrane potentials were measured in the following systems: Solution I|Supporting film| Solution II. All the membrane potentials were measured at 25 °C.

Theory and Method

Membrane Potential of Supporting Film. When a charged membrane separates electrolyte solution I and II whose concentration ratio C^{I}/C^{II} is R, the membrane potentials E are obtained by the summation of the diffusion potential in the membrane phase E^* and the Donnan potentials E_B at both interfaces;[16-18] they are expressed by the following equation:

$$E=E^{II}-E^{I}=(RT/F)((1/z_A)\ln R+(1/z_A)\ln(C^{II}/C^{I}) +((1/z_M-1/z_A)T_A^*-1/z_M)\times \ln((\bar{C}^{I}-(1/z_A)(1-T_A^*)\theta^*)/(\bar{C}^{II}-(1/z_A)(1-T_A^*)\theta^*)) \quad (1)$$

where θ^* and T_A^* are effective charge density of the membrane and the transference number of the anion in it. $\bar{C}_A^{I}$ and $\bar{C}_A^{II}$ are the interfacial concentration of the anion, and z_A and z_M are algebraic valences of the anion and the cation. The interfacial concentrations can be obtained by using the Donnan equilibrium between ions in the membrane phase and in bulk solutions, expressed by Eq. 2, and the electro-neutrality condition expressed by Eq. 3:

$$(\bar{C}_A/C_A)^{1/z_A}=(\bar{C}_M/C_M)^{1/z_M} \quad (2)$$

$$z_M\bar{C}_M+z_A\bar{C}_A+\theta^*=0 \quad (3)$$

Membrane Potentials of Multimembranes. The multimembrane, consisting of the polyelectrolyte solution sandwiched between supporting films, is shown in Fig. 1. The membrane potential E is the summation of the interfacial potentials generated at each interface of the multimembrane and the diffusion potential in each layer. According to the notations in Fig. 1 (b), E is expressed by the following equation:

$$E=\sum_{j=0}^{3}E_B^{j,j+1}+\sum_{j=1}^{3}E^{*j} \quad (4)$$

where $E_B^{j,j+1}$ and E^{*j} are the donnan potential at each interface and the diffusion potential in each layer respectively; the superscripts j and $(j,j+1)$ denote the jth layer and the interface between j and the $(j+1)$th layer respectively. The superscripts 0 and 4 denote Solution I and II, the first and third layers are supporting films, and the second one is the polyelectrolyte-solution layer. Denoting the concentration of the jth layer at the interface j and $(j+1)$th one by $\bar{C}^{j,j+1}$, and the effective charge density of the jth layer by θ^{*j}, E can be expressed by:

$$E=\frac{RT}{F}\left[\sum_{j=0}^{3}\ln\frac{\bar{C}_A^{j+1,j}}{\bar{C}_A^{j,j+1}}+\left\{\left(\frac{1}{z_M}+\frac{1}{z_A}\right)T_A^{*j}-\frac{1}{z_M}\right\}\times \sum_{j=1}^{3}\frac{\bar{C}_A^{j,j-1}+\frac{1}{z_A}(1-T_A^{*j})\theta^{*j}}{\bar{C}_A^{j,j+1}+\frac{1}{z_A}(1-T_A^{*j})\theta^{*j}}\right] \quad (5)$$

where T_A^{*j} is the transference number of the anion A in the jth layer. The Donnan equilibrium and the electro-neutrality conditions at each interface are expressed by the following equations:

$$(\bar{C}_A^{j+1,j}/\bar{C}_A^{j,j+1})^{1/z_A}=(\bar{C}_M^{j+1,j}/\bar{C}_M^{j,j+1})^{1/z_M} \quad (6)$$

$$z_M\bar{C}_M^{j,j+1}+z_A\bar{C}_A^{j,j+1}+\theta^{*j}=0 \quad (7)$$

$$z_M\bar{C}_M^{j+1,j}+z_A\bar{C}_A^{j+1,j}+\theta^{*j+1}=0 \quad (8)$$

j=0, 1, 2, and 3

where θ^{*0} and θ^{*4}, denoting the values of Solution I and II, are equal to 0. When θ^{*1} and θ^{*3} are known, $\bar{C}_A^{1,0}$ $\bar{C}_M^{1,0}$, $\bar{C}_A^{3,4}$, and $\bar{C}_M^{3,4}$ can be obtained by means of Eqs. 6—8 and as functions of C^{I} or C^{II}. Under steady state conditions, the fluxes of the ions J_i^j are equal in each layer, according to the continuity law:

$$J_i^1=J_i^2=J_i^3 \quad (9)$$

Approximating that concentrations of ions in each layer vary linearly,[19-21] the fluxes of the anion A are expressed by:

$$J_A^j=-P_A^j\frac{\bar{C}_A^{j,j+1}-\bar{C}_A^{j,j-1}}{l^j}(1+X) \quad (10)$$

$$X=\frac{\frac{z_M}{z_M-z_A}\theta^{*j}(\frac{1}{z_M}-\frac{1}{z_A})T_A^{*j}}{\bar{C}_A^{j,j+1}-\bar{C}_A^{j,j-1}}\times \ln\frac{\frac{z_M-z_A}{z_M}\bar{C}_A^{j,j+1}-(\frac{1}{z_M}-\frac{1}{z_A})(1-T_A^{*j})\theta^{*j}}{\frac{z_M-z_A}{z_M}\bar{C}_A^{j,j-1}-(\frac{1}{z_M}-\frac{1}{z_A})(1-T_A^{*j})\theta^{*j}} \quad (11)$$

j=1, 2, and 3

where P_A^j is the permeabiity coefficient of the anion in the j layer and where l^j is the thickness of the j layer. So as to satisfy Eq. 9, $\bar{C}_A^{1,2}$, $\bar{C}_A^{2,1}$, $\bar{C}_A^{2,3}$, and $\bar{C}_A^{3,2}$ can be obtained from Eq. 10 by numerical analysis. Then, the

membrane potentials E can be obtained from Eq. 5.

The effects of the supporting films on the membrane potential of the multimembrane can be discussed theoretically. Figures 2 and 3 show some of the calculated membrane potentials. The effects of the effective charge densities of the supporting films ($\theta^{*1}=\theta^{*3}$) on the membrane potentials are shown in Fig. 2. The effective charge density of the second layer is $\theta^{*2}=-0.01$ mol dm^{-3}, while those of the supporting films (θ^{*1} and θ^{*3}) vary from 0 to -0.1. The effects of θ^{*2} on E are shown in Fig. 3. The effective charge densities of the supporting films are $\theta^{*1}=\theta^{*3}=-0.01$ mol dm^{-3}, while that of the second layer varies from 0 to -0.1. In the calculations, Solution I and II are assumed to be NaCl solutions, and their ratio R to be 10. The P^{*1} ($=P^{*3}$) value is $1.92\cdot10^{-6}$ cm^2 s^{-1} which was obtained experimentally, and P^{*2} is $1.60\cdot10^{-5}$ cm^2 s^{-1}, which is approximated to be equal to the diffusion coefficient in an aqueous solution. The transference numbers of ions in membranes have been reported to be almost equal to those in their solutions.[16-18] Then, as the T_A^* value, the transference number of Cl^- in an NaCl solution was cited from the literature.[22] The thickness of the supporting films and the second layer are 0.0033 cm ($=l^1=l^3$) and 0.3 cm respectively, which are the same dimensions as those in the cell shown in Fig. 1 (a). It should be noted that the membrane potentials are affected not only by the effective charge densities of these layers but also by the diffusivities of ions through them. As the effective charge density of a supporting film θ^{*1} ($=\theta^{*3}$) drcreases under a constant θ^{*2}, as is shown in Fig. 2, the membrane potentials E are found to decrease abruptly in the lower-concentration region. When the θ^{*1} values are smaller than -0.001, the E values are almost the same; i.e., if θ^{*1} is at least smaller than one tenth of θ^{*2}, E is almost equal to those of $\theta^{*1}=0$. As is shown in Fig. 3, even when the θ^{*2} values are smaller than θ^{*1} ($=-0.01$), such as $\theta^{*2}=-0.001$ and -0.005, the differences between their membrane potentials are found to be clear, and even in these cases the θ^{*2} values can be obtained by the curve-fitting method.

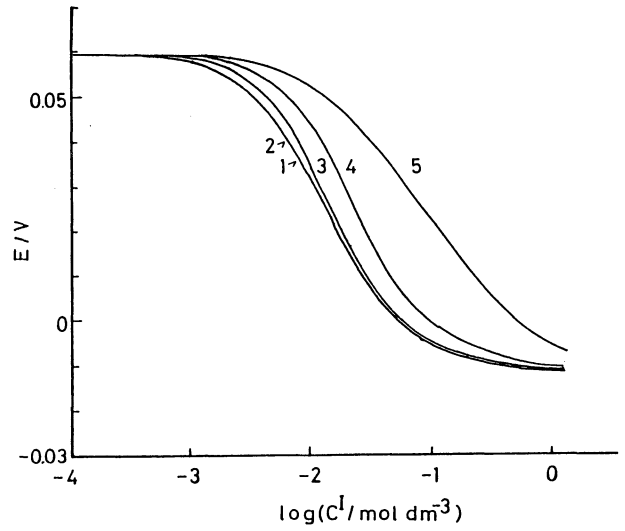

Fig. 2. Effects of effective charge densities of support film on membrane potentials E of multimembrane for NaCl solution at $R(=C^{I}/C^{II})=10$.
Effective charge densities of support films ($\theta^{*1}=\theta^{*2}$): 1; 0, 2; -0.0001, 3; -0.001, 4; -0.01, 5; -0.1.
Effective charge density of second layer θ^{*2}: -0.01.
Other data used in the calculations are as follows. $l^1=l^3=0.003$ cm, $l^2=0.3$ cm, $D^{*1}=D^{*3}=1.92\cdot10^{-6}$ cm^{2}s^{-1}, $D^{*2}=1.60\cdot10^{-5}$cm^{2}s^{-1}, $T_A{}^{*1}=T_A{}^{*2}=T_A{}^{*3}=0.601$.

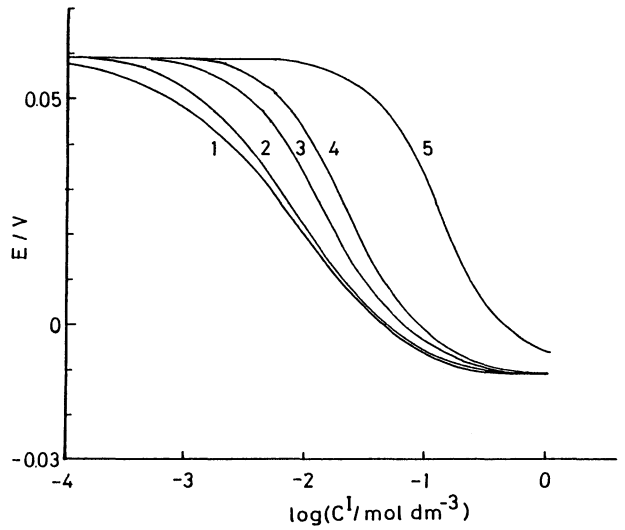

Fig. 3. Effects of effective charge densities of second layer on membrane potentials E of multimembrane for NaCl solution at $R=10$.
Effective charge densities of second layer θ^{*2}: 1; 0, 2; -0.001, 3; -0.005, 4; -0.01, 5; -0.1. Effective charge densities of support films $\theta^{*1}=\theta^{*3}$: -0.01. Other data used in the calculations are the same as in Fig. 2.

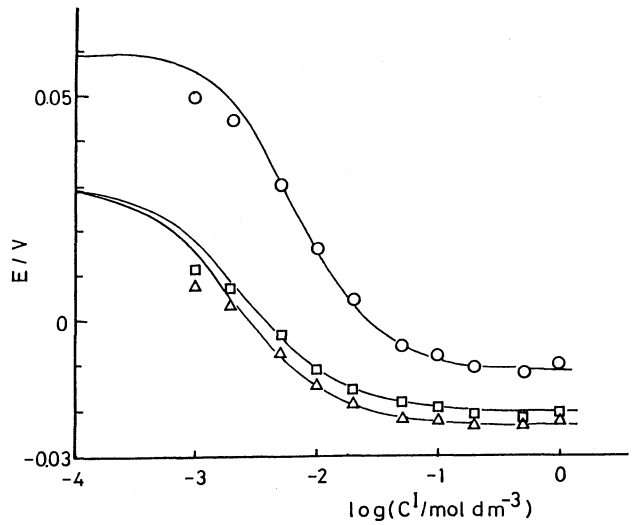

Fig. 4. Membrane potentials of support films for various electrolyte solutions at $R=10$.
○: NaCl, △: $MgCl_2$, □: $CaCl_2$. Solid curves show theoretical values obtained from Eq. 1 by selecting the most suitable effective charge densities.

Results

Effective Charge Density of Support Film. The membrane potentials of the supporting films C.M. were measured for NaCl, $MgCl_2$, and $CaCl_2$ solutions; the results are shown as functions of log C^I in Fig. 4. Their concentration ratios R ($=C^I/C^{II}$) were 10. The E values showed a shift from Donnan potentials to diffusion potentials with the increase in C^I. By the curve-fitting method, the effective charge densities of the film C.M., θ^*, were determined. The solid curves show the theoretical values obtained from Eq. 1 by selecting their most suitable values θ^* so as to agree with the experimental results in the high-concentration regions. In the calculations of the theoretical values, as the T_A^* values the transference numbers of the anion in the solutions were cited from the literature.[22] The θ^* values of the supporting film were found to be -0.0028, -0.0025, and -0.0026 mol dm^{-3} for NaCl, $MgCl_2$ and $CaCl_2$ solutions.

Effective Charge Densities of Alginates. The membrane potentials of the multimembranes (|Film C.M. |Alg Solution|Film C.M.|) were measured for the NaCl and $MgCl_2$ solutions, whose concentration ratio R was 10. The Alg solutions in the membrane ranged from W_{Alg}=0.00250 to 0.00262 g cm^{-3}. As is shown in Fig. 5, the E values showed abrupt decreases in the higher-concentration regions with the increase of W_{Alg}. The solid curves show the theoretical values obtained by selecting the most suitable values for the effective charge densities of alginate solutions, θ^{*2}, so as to agree with the experimental results. The θ^{*2} values are shown in Table 1, in which the effective

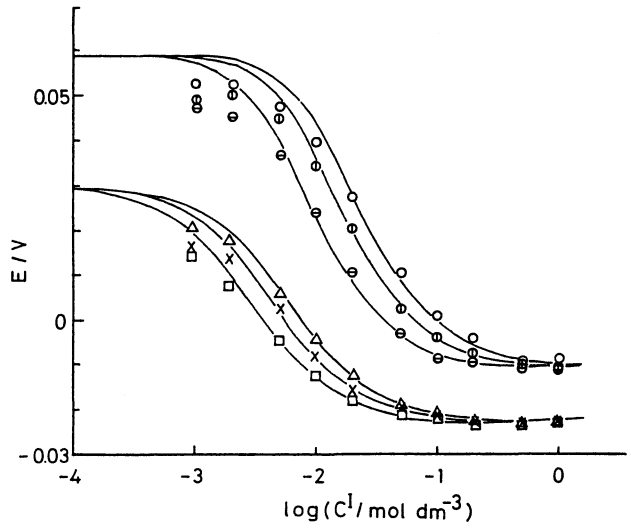

Fig. 5. Effects of concentration of Alg W_{Alg} on membrane potentials of multimembranes for NaCl and $MgCl_2$ solutions at R=10.
W_{Alg} (for NaCl solution): ○; 0.00626, ⊕; 0.00420, ⊖; 0.00250. W_{Alg} (for $MgCl_2$ solution): △; 0.00626, ×; 0.00420, □; 0.00250. Solid curves show theoretical values obtained by selecting the most suitable effective charge densities.

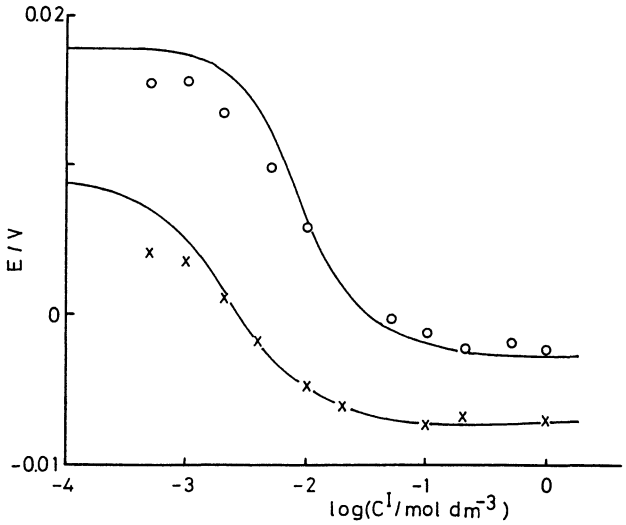

Fig. 6. Membrane potentials of multimembranes composed of alginate sol layer for NaCl and $MgCl_2$ solutions at R=2.
○; NaCl (W_{Alg}=0.00420), ×; $MgCl_2$ (W_{Alg}=0.00420). Solid curves show theoretical values obtained by selecting the most suitable effective charge densities.

Table 1. Characteristic Values of Alginate Sol and Gel

Solute	$-\theta^{*1}$/mol dm^{-3}	R	W_{Alg}/g cm^{-3}	$T_A^{*b)}$	$-\theta^{2*}$/mol dm^{-3}	θ^{2*}/θ_0
NaCl	0.0028	10	0.00626	0.601	0.014	0.44
NaCl	0.0028	10	0.00420	0.601	0.010	0.47
NaCl	0.0028	2	0.00420	0.601	0.010	0.47
NaCl	0.0028	10	0.00250	0.601	0.0050	0.40
$MgCl_2$	0.0025	10	0.00626	0.605	0.0080	0.25
$MgCl_2$	0.0025	10	0.00420	0.605	0.0065	0.31
$MgCl_2$	0.0025	2	0.00420	0.605	0.0060	0.28
$MgCl_2$	0.0025	10	0.00250	0.605	0.0035	0.28
$CaCl_2$[a)]	0.0026	10	0.00626	0.562	0.0035	0.11
$CaCl_2$[a)]	0.0026	10	0.00420	0.562	0.0025	0.12
$CaCl_2$[a)]	0.0026	10	0.00250	0.562	0.0015	0.12
NaCl[a)]	0.0028	10	0.00626	0.601	0.0070	0.22
NaCl[a)]	0.0028	2	0.00420	0.601	0.0060	0.28

a) CaAlg gelled by 1.0 mol dm^{-3}. b): $T_A^*=T_A^{*1}=T_A^{*2}=T_A^{*3}$. θ^{*1}: charge density of supporting film C.M.($=\theta^{*3}$). θ^{*2}: charge density of Alg. θ_0: concentration of Alg on the basis of uronate units.

charge densities of the supporting films C.M. θ^{*1} ($=\theta^{*3}$) and the transference numbers of the anion T_A^{*j} used in calculations are also shown. The absolute values θ^{*2} for the NaCl solution were bigger than those for $MgCl_2$, and they increased with the increase in W_{Alg}. Figure 6 shows the membrane potentials for the NaCl and $MgCl_2$ solutions, whose concentration ratio R was 2. The most suitable θ^{*2} values of Alg are shown in Table 1, also. They were in good agreement with the θ^{*2} values obtained when R=10.

In the cases of the NaCl and $MgCl_2$ solutions, the Alg were in sol states, but in the case of the $CaCl_2$ solutions they were in the gel state. The membrane potentials of the Alg in the gel state were measured as follows. The Alg sols (NaAlg) in the second layer were transited to gel by putting $CaCl_2$ solutions (1.0 mol dm^{-3}) into both compartments, I and II, and before the measurements of E, the free ions in the CaAlg gel layer were removed by dialysis against distilled water. Figure 7 shows the membrane potentials of the multimembranes containing CaAlg gels for NaCl and $CaCl_2$ solutions (R=10) and also the theoretical curves obtained by using the most suitable effective charge densities θ^{2*}, which are shown in Table 1. The absolute values of the effective charge density of CaAlg were found to be less than those of MgAlg. This is attributable to the capture of the Ca ion in the junctions. The absolute values of θ^{*2} of CaAlg for NaCl-solution systems were bigger than those for $CaCl_2$ solutions. This is considered to result from the partial ion-exchange of Ca with Na ions.

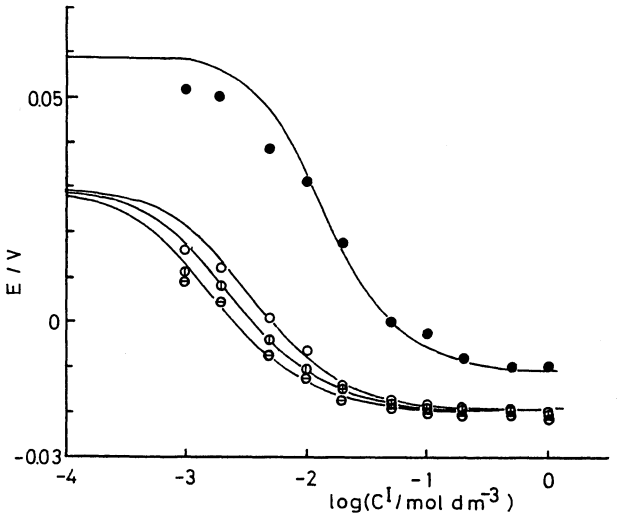

Fig. 7. Membrane potentials of multimembranes composed of alginate gel layer for NaCl and $CaCl_2$ solutions at R=10.
W_{Alg} (for $CaCl_2$ solution): ○; 0.00626, ⊕; 0.00420, ⊖; 0.00250. W_{Alg} (for NaCl solution): ●; 0.00626.

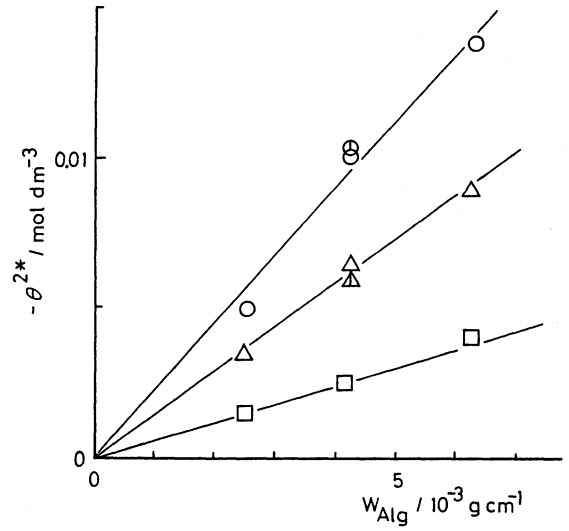

Fig. 8. Effective charge densities vs. concentrations of alginates. NaAlg: ○ (R=10), ⊕ (R=2). MgAlg: △ (R=10), ▲ (R=2). CaAlg: □ (R=10).

Figure 8 shows the effective charge densities of alginates as a function of the concentration of alginates W_{Alg}. As W_{Alg} increases, the absolute values increase almost linearly; their magnitudes were as follows; Na->Mg->Ca-Alg.

Discussion

Counterion-Binding Characteristics of Alginates. The concentration of Alg based on the uronate units, which corresponds to the concentration of carboxyl groups C_{car} mol dm^{-3}, is obtained by the use of Eq. 12. If all the carboxyl groups work as charged groups, the absolute value of the charge density of Alg is equal to C_{car}:

$$C_{car}=|\theta_0|=10^3\, W_{Alg}/M_u, \qquad (12)$$

where M_u is the molar mass of the uronates. The ratios of the effective charge density of Alg to θ_0, θ^{*2}/θ_0, show the fractions of the ionized carboxyl groups. The W_{Alg} in the second layer might decrease because of osmotic pressures. However, by the help of the perforated support plates (F) shown in Fig. 1 (a), we estimate that the decrease in W_{Alg} could be neglected. As is shown in Table 1, the θ^{*2}/θ_0 values were found not to depend remarkably on W_{Alg} in the experimental region. The mean θ^{*2}/θ_0 values for Na-, Mg-, and CaAlg were 0.45, 0.28, and 0.12 respectively. Na- and MgAlg were in sol states. The interactions of Na^+ and Mg^{2+} with Alg were dominantly electrostatical. Therefore, the differences in their values θ^{*2}/θ_0 can be surmised to result from their valence effects. Ca ions mediate the stackings of Alg molecules to form the junctions.[2-4] Then, the much smaller value of CaAlg than MgAlg results from the constraints of Ca ions in the junctions and in the networks.

Alg can be considered to behave as a rod like polyelectrolyte in diluted solutions, because of the electrostatical repulsive force between the charged groups and the rigidity of their saccharide structure. Manning's theory[23,24] is appropriate for discussing the thermodynamic quantities of rod like polyelectrolytes in diluted solutions.[25-30] By comparing our results with the

theoretical results, the effects of the polymer-polymer interactions and the network formations on counterion bindings can be discussed. In theory, the interaction of polyelectrolytes with counterions are considered to be of two modes: the Debye-Hückel ion atmosphere and the condensation on charged groups. The key parameter, ξ, for the counterion condensation in Manning's theory is defined by Eq. 13 and is proportional to the line charge density,[23,24] i.e., the reciprocal of the distance between the neighbouring charged groups b:

$$\xi = e^2/(4\pi\varepsilon kTb) \quad (13)$$

where e is the protonic charge and where ε is the permitivity of the solvent. The b value of NaAlg has been reported to be 0.497 nm, and the ξ value, 1.43.[31] The osmotic coefficients ϕ_M of salt-free polyelectrolytes are expressed by:

$$\phi_M = 1/(2z_i\xi) \quad (14)$$

The theoretical ϕ_M values of Alg with monovalent and divalent counterions are 0.35 and 0.17. The ϕ_M value can be considered approximately to be the degree of ionization of the charged groups in polymers.[32] By comparing the experimental θ^{*2}/θ_0 values shown in Table 1 with the ϕ_M values, we can see that both results for Na- and MgAlg were much larger than the ϕ_M values. Kobatake et al.[11] discussed precisely the thermodynamical and hydrodynamical effective charge densities of Poly (styrenesulfonate) (PSS) solutions by using the membrane-potential and Donnan-potential methods. Their θ^{*2}/θ_0 values of potassium salt of PSS (KPSS) obtained from the membrane potential were reported to be 0.4. As the theoretical value ϕ_M of KPSS is 0.18,[24] the effective charge density was also much greater than the ϕ_M value. It is a significant problem that the effective charge densities of polyelectrolyte solutions are much greater than the ϕ_M values. This might be the effect of the hydrodynamical effects described by Kobatake et al.[11]

Effects of Gellation on Ca-Ion Bindings. The electrostatical interactions of Mg and Ca ions with Alg are assumed to be equal. Then, the difference in θ^{*2}/θ_0 between Mg- and CaAlg, $|(\theta^{*2}(\text{MgAlg}) - \theta^{*2}(\text{CaAlg}))/\theta_0| = 0.16$, shows the ratio of the enhanced Ca-ion bindings due to the gellation of Alg. Whether this increase results primarily from the entrapping of Ca ions in the junctions should be discussed. When the fraction of the junctions in a Alg molecule is F_j, on the basis of the concentration of the uronate units, and when the Ca-ion binding ratio in the junctions and in the Alg chains between the junctions are $(\sigma_j)_{Ca}$ and $(\sigma_i)_{Ca}$, the fraction of ionized carboxyl groups in CaAlg gels $(\theta^{*2}/\theta_0)_{Ca}$ can be expressed by the following equation:

$$(\theta^{*2}/\theta_0)_{Ca} = F_j(1-(\sigma_j)_{Ca}) + (1-F_j)(1-(\sigma_i)_{Ca}). \quad (15)$$

The Ca ions entrapped in the junctions can be assumed to bind completely to Alg,[33] i.e., $(\sigma_j)_{Ca}=1$, and all GG blocks are assumed to contribute to the formation of the junctions, i.e., $F_j = F_{GG} = 0.28$. Under these assumptions, the value $(\sigma_i)_{Ca}$ of CaAlg is calculated from the result $(\theta^{*2}/\theta_0)_{Ca}$ (=0.12); it is 0.83, which is bigger than the Mg-ion-binding ratio σ_{Mg} (=$(1-(\theta^{*2}/\theta_0)_{Mg}$=0.72). Actually, F_j is considered to be smaller than F_{GG}. Therefore, $(\sigma_i)_{Ca}$ should be bigger than 0.83. From these considerations, it can be concluded that the Ca-ion bindings are enhanced by the gellation not only in the junction, but even in the regions between the junctions, i.e., in the networks.

References

1) A.Haug, B. Larsen, and O. Smidsrod, *Carbohydr. Res.*, **32**, 217 (1974).
2) D. A. Rees, *Biochem. J.*, **126(2)**, 257 (1972).
3) E. R. Morris, D. A. Rees, and D. Thom, *Carbohydr. Res.*, **66**, 143 (1978).
4) T. A. Bryce, A. A. McKinnon, E. R. Morris, D. A. Rees, and D. Thom, *Faraday Discuss. Chem. Soc.*, **57**, 221 (1974).
5) A. Suggett, "Water," ed by F. Franks, Vol. 4, Plenum Press, New York (1975), p. 519.
6) Y. F. Leung, G. M. O'Shea, M. F. A. Coosen, and A. M. Sun, *Artif. Organs*, **7(2)**, 208 (1983).
7) H. Tanaka, M. Matsumura, and I. A. Veliky, *Biotechnol. Bioeng.*, **26**, 53 (1984).
8) R. Kohn, I. Furda, A. Haug, and O. Smidsrod, *Acta Chem. Scand.*, **22**, 3098 (1968).
9) O. Smidsrod, and A. Haug. *Acta Chem. Scand.*, **22**, 1989 (1968).
10) A. Haug, and O. Smidsrod, *Acta Chem. Scand.*, **24**, 843 (1970).
11) M. Yuasa, Y. Kobatake, and H. Fujita, *J. Phys. Chem.*, **72(8)**, 2871 (1968).
12) E. R. Morris, D. A. Rees, and D. Thom, *Carbohydr. Res.*, **81**, 305 (1980).
13) H. Grasdalen, B. Larsen, and O. Smidsrod, *Carbohydr. Res.*, **68**, 23 (1979).
14) M. Yonese, *Hyoumen*, **18**, 692 (1980).
15) J. Kielland, *J. Am. Chem. Soc.*, **59**, 1675 (1937).
16) N. Takeguchi and M. Nakagaki, *Biochim. Biophys., Acta*, **219**, 405 (1970).
17) M. Nakagaki and K. Miyata, *Yakugaku Zasshi*, **93**, 1105 (1973).
18) M. Yonese and M. Nakagaki, *Yakugaku Zasshi*, **96**, 299 (1976).
19) P. Henderson, *Z. Physik. Chem.*, **59**, 118 (1907).
20) M. Nakagaki and M. Kobayashi, *Yakugaku Zasshi*, **93**, 964 (1973).
21) M. Nakagaki and R. Takagi, *Membranes*, **4**, 183 (1979).
22) R. Parsons, "Handbook of Electrochemical Constants," Butterworths Scientific Publications, London (1959), p. 87.
23) G. S. Manning, *Annu. Rev. Phys. Chem.*, **23**, 117 (1972).
24) G. S. Manning, "Charged and Reactive Polymers I, Polyelectrolytes," ed by E. Selegny, D. Reidel Publishing Co., Boston (1972), p. 9.
25) M. Yonese, H. Tsuge, and H, Kishimoto, *Nippon Kagaku Kaishi*, **1978**, 108.

26) H. Tsuge, M. Yonese, and H. Kishimoto, *Bull. Chem. Soc. Jpn.*, **52**, 2846 (1979).
27) M. Yonese, H. Tsuge, and H. Kishimoto, *Bull. Chem. Soc. Jpn.*, **54**, 20 (1981).
28) H. Tsuge, M. Yonese, and H. Kishimoto, *Nippon Kagaku Kaishi*, **1978**, 609.
29) H. Tsuge, M. Yonese, and H. Kishimoto, *Nippon Kagaku Kaishi*, **1982**, 1583.
30) M. Yonese, H. Tsuge, and H. Kishimoto, *J. Phys. Chem.*, **91**, 1971 (1987).
31) T. J. Podlas and P. Ander, *Macromolecules*, **3**, 154 (1970).
32) M. Nakagaki, S, Shimabayashi, E. Hayakawa, and T. Kotsuki, *Yakugaku Zasshi*, **99**, 618 (1979).
33) A. Katchalsky, R. E. Cooper, J. Upadhyay, and A. Wassermann, *J. Chem. Soc.*, **1961**, 5198.
34) R. Kohn and B. Larsen, *Acta Chem. Scand.*, **26**, 2455 (1972).